Galactose Oxidase as a Mode l for Reactivity at a Copper Superoxide Center

Kristi J. Humphreys[‡,Δ], **Liviu M. Mirica**[‡,^], **Yi Wang**[‡,#], and **Judith P. Klinman**[‡,†,*]

‡*Department of Chemistry, University of California, Berkeley, California 94720, USA.*

†*Departments of Molecular and Cell Biology, University of California, Berkeley, California 94720, USA.*

Abstract

The mononuclear copper enzyme, galactose oxidase, has been investigated under steady-state conditions via O_2-consumption assays using 1-O-methyl-α-D-galactopyranoside as the sugar substrate to produce an aldehyde at the C-6 position. The rate-determining step of the oxidative half-reaction was probed through the measurement of substrate and solvent deuterium and O-18 isotope effects on $k_{cat}/K_m(O_2)$. The reaction conforms to a ping-pong mechanism with the kinetic parameters for the reductive half, $k_{cat}/K_m(S) = 8.3 \times 10^3$ M^{-1} s^{-1} at 10°C and pH 7.0, comparing favorably to literature values. The oxidative half-reaction yielded a value of $k_{cat}/K_m(O_2) = 2.5 \times 10^6$ M^{-1} s^{-1}. A substrate deuterium isotope effect of 32 was measured for the $k_{cat}/K_m(S)$, while a smaller, but significant value of 1.6-1.9 was observed on $k_{cat}/K_m(O_2)$. O-18 isotope effects of 1.0185 with either protiated or deuterated sugar, together with the absence of any solvent isotope effect, lead to the conclusion that hydrogen atom transfer from reduced cofactor to a Cu(II)-superoxo intermediate is fully rate-determining for $k_{cat}/K_m(O_2)$. The measured O-18 isotope effects provide corroborative evidence for the reactive superoxo species in the dopamine β-monooxygenase/peptidylglycine α-hydroxylating monooxygenase family, as well as providing a frame of reference for copper-superoxo reactivity. The combination of solvent and substrate deuterium isotope effects rules out solvent deuterium exchange into reduced enzyme as the origin of the relatively small substrate deuterium isotope effect on $k_{cat}/K_m(O_2)$. These data indicate fundamental differences in the hydrogen transfer step from the carbon of substrate vs. the oxygen of reduced cofactor during the reductive and oxidative half reactions of galactose oxidase.

Keywords

Copper superoxo reactivity; galactose oxidase; oxidative half reaction; deuterium; O-18 isotope effects

1. Introduction

Galactose oxidase (GAOX) has been the subject of extensive study over a period of several decades. Interest in this extracellular copper enzyme was initially fueled by the mystery surrounding the prospect of a two-electron oxidation/reduction mediated by a single copper atom. Recent interest, however, can be attributed to the discovery of the enzyme's protein-derived radical cofactor (TyrCys) formed via cross-linking of an active site tyrosine to cysteine.

*To whom correspondence should be addressed. Tel: 510-642-2668; Fax: 510-643-6232; E-mail: E-mail: klinman@berkeley.edu..
ΔCurrent address: Department of Chemistry, Dickinson College, P.O. Box 1773, Carlisle, PA 17013.
^Current address: Department of Chemistry, Washington University at St. Louis, 1 Brookings Drive, St. Louis, MO 63130-4899
#Current address: HIV Drug Resistance Program, NCI-Frederick, P.O. Box B, 1050 Boyles Street, Building 535, Room 325, Frederick, MD 21702-1201.

[1,2] GAOX catalyzes the oxidation of a broad range of primary alcohols to their corresponding aldehyde. Stopped flow studies have demonstrated that the net reaction can be separated into two half-reactions,[3,4] the first of which involves substrate oxidation and reduction of the enzyme to yield Cu(I)-tyrosinate, eq. (1):

$$E - B{:}^- + Cu^{II} - (\bullet O - TyrCys) + RCH_2OH \rightarrow E - BH + Cu^I - (HO - TyrCys) + RCHO \tag{1}$$

This process can be further broken down into three steps: proton transfer from substrate to an active site base, hydrogen atom transfer to the cofactor-based radical center, and electron transfer to the Cu(I), Scheme 1A. A large kinetic isotope effect has been observed on the rate of sugar oxidation, ascribed to H-atom tunneling from substrate to cofactor.[3]

Considerably less is known about the oxidative process resulting in production of hydrogen peroxide from dioxygen and regeneration of the radical cofactor and Cu(II), eq. (2):

$$E - BH + Cu^I - (HO - TyrCys) + O_2 \rightarrow E - B{:}^- + Cu^{II} - (\bullet O - TyrCys) + H_2O_2 \tag{2}$$
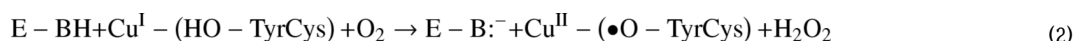
Analogous to the reductive half reaction, a three-step mechanism can be proposed for the recycling of reduced enzyme (Scheme 1B). In the first step, electron transfer from Cu(I) to coordinated oxygen yields metal-bound superoxide. In a second step, metal-bound superoxide abstracts a hydrogen atom from the phenolic hydroxyl group of the TyrCys cofactor to produce hydroperoxide and TyrCys•. Finally, a proton is transferred from the axial tyrosine to metal-bound hydroperoxide to produce hydrogen peroxide and fully re-oxidized enzyme.

Historically, the superoxide ion had been considered too "sluggish" an oxidant, relative to peroxide and hydroxyl radical, for efficient H-atom abstraction. In this context, there has been lengthy debate over the possible activated oxygen intermediates utilized by the copper enzymes, dopamine β–monooxygenase (DβM) and peptidylglycine α-hydroxylating monooxygenase (PHM), during substrate hydroxylation.[5-8] Most recently, these enzymes have been concluded to employ a mono-nuclear cupric superoxide ion, based on extensive steady-state kinetics data that include deuterium and O-18 isotope effects and product analyses that implicate full coupling between dioxygen and substrate uptake.[9,10] DFT calculations have provided strong support for the involvement of a metal superoxide complex as the hydroxylating agent,[11] while X-ray studies of PHM, characterized in the presence of a slow substrate and O_2, indicate a bound oxygen species that may well be superoxide ion.[12] As introduced above, consideration of possible mechanisms for reaction of reduced GAOX with O_2 points toward initial formation of a superoxide intermediate via electron transfer from Cu (I) to dioxygen. Further, the fact that hydrogen peroxide is the product of the galactose oxidase reaction makes superoxide the only reasonable mediator of H-atom abstraction from reduced cofactor. We, thus, present GAOX as an ideal system in which to investigate the properties of superoxide reactivity at enzymatic mononuclear copper centers.

Steady-state kinetics that include substrate and solvent deuterium and O-18 kinetic isotope effects can provide remarkable insight into the rate-controlling step(s) in O_2-utilizing enzymes as well as, in selected cases, the nature of reactive oxygen intermediates. Comparison of the present kinetic results for GAOX to data for PHM and DβM provides corroborative evidence in support of the proposed superoxo- intermediate in the latter systems. In particular, the size of the O-18 KIE provides a frame of reference for the reactivity of $Cu(II)(O_2{\cdot}^-)$ in both oxidase and oxygenase-type enzymes. These studies also allow comparison of the impact of substrate deuteration on the properties of alcohol oxidation (C-H abstraction) vs. O_2 reduction (O-H activation) within a single enzyme active site.

2. Experimental

Materials and Methods

1-O-methyl-α-D-galactopyranoside (H_2-OMeGal), catalase, potassium ferricyanide, 3-methoxybenzyl alcohol, and D_2O were purchased from Sigma-Aldrich and used without further purification. The 1-O-methyl-[6,6-$^2H_2$]-α-D-galactopyranoside (D_2-OMeGal) substrate was synthesized according to the literature.[3] Ferricyanide stock solutions were prepared fresh daily. GAOX was found to be highly sensitive to contaminants on the surface of glass- and plasticware. Vessels used during the fungal growth and enzyme purification steps were rinsed three times with de-ionized water prior to use. GAOX was stored at −80 °C in DNase/RNase- and pyrogen-free microcentrifuge tubes (USA Scientific). Activated GAOX was stored in glass vials that had been washed with hexanes, 6 M nitric acid, de-ionized water, and methanol, then dried in an oven. The cuvettes for spectroscopic assays were rinsed with 1 M nitric acid, de-ionized water and methanol, then thoroughly dried.

Purification and Isolation of GAOX

GAOX was isolated from the growth medium of the fungus, *D. dendroides*, (spp. *Fusarium*, ATCC 46032) and purified according to the literature procedure of Tressel and Kosman.[13] Exceptions to this protocol are as follows: catalase (10 mg/L) was added to the dialysis buffer during the exchanges into 10 mM sodium phosphate (pH 7.0) and 100 mM sodium acetate (pH 7.2).[14] Following batch-processing with DEAE, the filtrate was concentrated, dialyzed against 100 mM sodium acetate (pH 7.2) and then purified via affinity chromatography on sepharose 6B.[15] GAOX was eluted from the column in the same buffer. The fractions were subjected to denaturing gel electrophoresis (10% SDS-PAGE) and analyzed for concentration and specific activity using UV-vis spectroscopy. Fractions containing GAOX at a constant specific activity were pooled and dialyzed against 50 mM sodium phosphate (pH 7.0). Dialyzed protein was concentrated under pressure to 3 mg/mL, assayed for specific activity and O_2 consumption, and then snap-frozen in $N_2(l)$ for storage at −80 °C. Prior to use, GAOX stored at −80 °C was thawed on ice, mixed by pipet and assayed for concentration, specific activity, and O_2 consumption.

Concentration and Specific Activity

The concentration of GAOX was determined using published extinction coefficients at 280 nm of 1.05×10^5 $M^{-1}cm^{-1}$ and 1 OD = 0.65 mg/ml.[16] Specific activity was measured at pH 7.0 and 25 °C using 60 mM 3-methoxybenzyl alcohol as the substrate. The extinction coefficient of the 3-methoxybenzaldehyde product is $\Delta\varepsilon = 2691$ $M^{-1}cm^{-1}$,[13] providing a rapid spectroscopic method to determine activity levels.

Activation

As isolated GAOX is a mixture of active enzyme possessing TyrCys• and inactive enzyme wherein the TyrCys radical has been reduced. In order to obtain a homogeneous sample of active radical-containing enzyme, GAOX was activated by brief incubation with 1:10 volume of enzyme: 50 mM $K_3Fe(CN)_6$ followed by purification on a MicroBioSpin P-6 column.[17] Protein eluted from the column was mixed by pipet then assayed for concentration and specific activity.

Steady-state Measurements

Oxygen uptake experiments were conducted using a Clark type electrode (YSI). For measurements conducted at less than or equal to 350 μM O_2, the electrode was calibrated using the concentration of dissolved oxygen in water under air-saturating conditions at 10 °C (1V = 352 μM). For measurements taken at greater than 350 μM O_2, the electrode was calibrated with

100% O_2 at 10 °C (1V = 1686 μM). Reaction volumes were 1 mL with final concentrations of 50 mM sodium phosphate (pH 7.0), 1-500 mM H_2-OMeGal and 1 mM $K_3(FeCN)_6$. Ferricyanide was included in the reaction mixture to ensure full enzyme activity. Stock solutions of the sugar and ferricyanide were prepared in 50 mM sodium phosphate (pH 7.0) and adjusted for pH. After equilibration of the reaction mixture at 10 °C and the desired concentration of O_2 (40-1000 μM), 1-4 μL of 2 μM activated enzyme was added via syringe. The reaction was monitored by following the change in concentration of dissolved O_2 with respect to time. To minimize variability in O_2 consumption rates between enzyme aliquots, a standard reaction under air-saturating conditions with 50 mM substrate and 4 nmol GAOX was measured daily and normalized to 225 s^{-1}. All subsequent measurements collected on a given day were adjusted according to the ratio obtained from the standard reaction.

Kinetic Isotope Effects

Experiments with deuterated substrate, D_2-OMeGal, were carried out at 10 °C in 50 mM sodium phosphate (pH 7.0) and 1 mM $K_2Fe(CN)_6$. The sugar concentration was maintained at 200 mM while O_2 concentration was varied between 12 and 350 μM utilizing a mixture of N_2(g) and air.

pH Dependence of Oxidative Half-Reaction

The effect of pH on $k_{cat}/K_m(O_2)$ was evaluated under steady-state conditions at 10 different pH values (pH 6-8, 50 mM sodium phosphate, pH 8-9, 20 mM sodium pyrophosphate, pH 9-10.5, 100 mM glycine/NaOH). The concentration of H_2-OMeGal was held constant at 200 mM while $[O_2]$ was varied from 40-350 μM.

Solvent Isotope Effects

The solvent isotope effect on $k_{cat}/K_m(O_2)$ was measured under steady-state conditions in D_2O at 7 different pD values (pD 6-8, 50 mM sodium phosphate, pD 8-9, 20 mM sodium pyrophosphate). The concentrations of H_2-OMeGal and O_2 were the same as in the experiments at varying pH values. Stock solutions were prepared by dissolving the buffer salts and H_2-OMeGal in D_2O and then lyophilizing. Following a second lyophilization the samples were re-dissolved in D_2O to the desired concentration and adjusted to the appropriate pD using NaOD or D_3PO_4. The pD was determined by measuring the pH and adding 0.4 to the value.

[18]O Isotope Effects

[18]O kinetic isotope effects (KIEs) were measured competitively as described previously.[18,19] Reactions with GAOX (0.5-8 nM) were carried out in 50 mM sodium phosphate (pH 7.0) at 10 °C with ~1 mM O_2 and 50 mM H_2-OMeGal or D_2-OMeGal. The reaction was coupled with horseradish peroxidase (200 nM) using guaiacol (3 mM) as the substrate to convert H_2O_2 to H_2O. The ^{18}O/^{16}O ratios of residual oxygen were measured using isotopic ratio mass spectrometry (Department of Earth and Planetary Science, UC Berkeley, CA). The [18]O KIEs are expressed as a ratio of ratios according to eq (1), where R_f is the ^{18}O/^{16}O isotopic ratio of substrate at f fractional conversion and R_0 is the isotopic ratio of the blank.

$$\frac{R_f}{R_0} = (1-f)^{\left(\frac{1}{^{18}OKIE}\right)-1}$$

(3)

Calculation of [18]O Equilibrium Isotope Effects

The equilibrium isotope effects (EIEs) can be expressed as a product of three terms, contributed from the zero-point energies (ZPE), excited vibration states (EXC), and the mass and moments

of inertia (MMI): EIE = ZPE × EXC × MMI.[18] All three terms are related to vibrational frequencies of $^{18}O-$ and $^{16}O-$containing reactants and products, as described previously.[19] For the Cu(II)(OOH) species, Cu-O and O-O experimental frequencies were used to calculate the ^{18}O EIEs given in Table 3, in a manner similar to previous reports.[20] The populations of the two possible isotopic distributions (e.g. $Cu^{II}-^{18}O^{16}OH$ or $Cu^{II}-^{16}O^{18}OH$) are expected to be close to each other, hence the ^{18}O EIE was calculated using the formula: $^{18}EIE_{calc} = 2/(^{18,16}K^{-1} + ^{16,18}K^{-1})$.[19] For the Cu(II)(OOH) species, the frequencies and isotope shifts used for the O-H stretch and O-O-H bending modes were taken from Tian et al.[19]

3. Results

Expression and Purification

Analysis of purified GAOX by denaturing gel electrophoresis (10 % SDS-PAGE) yielded a band accounting for greater than 95 % of the sample with an estimated molecular weight of 65 kD, consistent with the reported mobility for mature enzyme.[21] All of the enzyme aliquots stored at −80 °C yielded the same concentration and specific activity after thawing. Following activation, the aliquots produced an average specific activity of 150 U/mg using the 3-methoxy benzyl alcohol assay, in accordance with reported literature values of 140 and 166 U/mg.[22,23] The 3-methoxy benzyl alcohol assay provided a quick and easily comparable spectrophotometric method for assessing the condition and activity of GAOX before proceeding with kinetics measurements utilizing the more reactive 1-O-methyl-α-D-galactopyranoside as the substrate.

Steady-State Kinetics

Steady-state kinetics information was obtained by measuring the rate of O_2 consumption at a constant oxygen concentration while varying the H_2-OMeGal concentration between 1 and 500 mM. Plots of the rate of O_2 consumption (s^{-1}) versus substrate concentration (mM) were fitted to the Michaelis-Menten equation and showed that both $k_{(app)}$ and K_m for the sugar increased at higher oxygen concentrations, while the value of k_{cat}/K_m for sugar remained constant. The rate of O_2 consumption vs. O_2 concentration was analyzed as a function of varied substrate in a similar fashion, yielding values for $k_{cat}/K_m(O_2)$ that remained independent of sugar concentration. The latter feature is illustrated by a reciprocal plot of $1/k_{(app)}$ vs. $1/[O_2]$ at 5 different sugar concentrations yielding a series of parallel lines with slopes equal to $K_m/k_{cat}(O_2)$, Figure 1. The limiting value of k_{cat} at saturating oxygen and substrate, as well as $k_{cat}/K_m(OMeGal)$ at saturating oxygen and $k_{cat}/K_m(O_2)$ at saturating sugar are given in Table 1.

Deuterium Isotope Effects

Steady-state kinetic measurements were conducted with substrate that was dideuterated at position C-6 to assess the extent to which hydrogen atom transfer is involved in the rate-determining step of the oxidative half-reaction. Rate measurements vs. varying $[O_2]$ were carried out at a single concentration of D_2-OMeGal (200 mM), giving an apparent k_{cat} of $23.1 \pm 0.4 \ s^{-1}$, a K_m for O_2 of $15 \pm 2 \ \mu M$ and a $k_{cat}/K_m(O_2)$ of $1.5 \pm 0.2 \times 10^6 \ M^{-1}s^{-1}$. Alternatively, keeping $[O_2]$ at 350 μM, rates were measured at variable $[D_2$-OMeGal,$]$ giving a k_{cat} of $49 \pm 2 \ s^{-1}$, a K_m for D_2-OMeGal of $1.90 \pm 0.2 \times 10^2$, and a $k_{cat}/K_m \ (D_2$-OMeGal$)$ of $2.6 \pm 0.4 \times 10^2 \ M^{-1}s^{-1}$. The resulting small substrate deuterium isotope effect on $k_{cat}/K_m(O_2)$ (to be discussed later), together with the large isotope effect on k_{cat}, leads to a significantly reduced K_m for O_2 when using deuterated sugar. Thus, an experimental oxygen concentration of 350 μM is high enough to ensure O_2 saturation leading to an excellent approximation of the true k_{cat} and $k_{cat}/K_m(D_2$-OMeGal$)$ at saturating $[O_2]$, Table 1. By contrast, the analysis of rate vs. $[O_2]$ at about K_m concentration for D_2-OMeGal is expected to provide a plateau region approximately one-half k_{cat}, compatible with the observed value of 23.1 s^{-1}. Given the ping-

pong nature of the reaction (cf. Figure 1) the values for $k_{cat}/K_m(H_2\text{-OMeGal})$ and $k_{cat}/K_m(O_2)$ and their respective isotope effects will be independent of the concentration of the alternate substrate. The isotope effects resulting from deuterated substrates are in Table 2. We note that Whittaker et al.[3] had earlier reported a limiting deuterium isotope effect of 8 ± 1 at saturating substrate and a single concentration of O_2. While this was attributed to the O_2 half reaction, the ca. 6-fold reduction in the $K_m(O_2)$ value for deuterio- substrate (cf. Table 1) obviates any clear-cut mechanistic conclusion regarding the role of substrate-derived deuterium in the oxidative half reaction.

The involvement of proton transfer in the rate-determining step of the oxidative half-reaction was assessed through steady-state measurements in D_2O at a constant level of sugar, 200 mM H_2-OMeGal. At a pD of 7.0, $k_{cat}/K_m(O_2)$ was $2.5 \pm 0.7 \times 10^6$ $M^{-1}s^{-1}$ yielding a solvent isotope effect of 1.0. Experiments utilizing deuterated sugar in D_2O resulted in $k_{cat}/K_m(O_2) = 1.3 \pm 0.3 \times 10^6$ $M^{-1}s^{-1}$ and a "double" kinetic deuterium isotope effect of 1.9.

pH Effect

Measurements of $k_{cat}/K_m(O_2)$ at pH values between 6 and 10.5 were utilized to evaluate the involvement of ionizable groups in the rate-determining step of the oxidative half-reaction. Varying the pH in increments of 0.5 pH units revealed a maximum in $k_{cat}/K_m(O_2)$ between pH 6.5 and 7.5 (Figure 2). Increasing the pH from 7.5 to 10.5 resulted in a decrease of $k_{cat}/K_m(O_2)$ by approximately 2 orders of magnitude. The plot of log $k_{cat}/K_m(O_2)$ versus pH was fitted to an acidic and basic pK_a ($pK_{a1} = 5.4(0.3)$ and $pK_{a2} = 8.76(0.04)$). When the pD was varied between 6.0 and 9.0, a maximum was seen in log $k_{cat}/K_m(O_2)$ between pD 7.0 and 8.0. Below pD 7.0 and above pD 8.0, a decrease in log $k_{cat}/K_m(O_2)$ was observed ($pK_{a1} = 6.1(0.1)$ and $pK_{a2} = 9.14(0.05)$). The overall profile obtained by varying pD is similar to that seen from varying the pH except that the curve is shifted to the right, along the x-axis.

^{18}O Isotope Effects

To obtain additional information on the interaction of reduced GAOX with O_2 to produce hydrogen peroxide and oxidized GAOX, the ^{18}O kinetic isotope effects (^{18}O KIEs) were measured. Competitive ^{18}O KIEs were determined from the fractionation of oxygen isotopes, i.e. the change in $^{18}O/^{16}O$ during the consumption of O_2 catalyzed by GAOX. Isotope fractionation plots ($^{18}O/^{16}O$ isotopic ratios of ratios versus fractional conversion) for the reduction of O_2 by GAOX using H_2-OMeGal and D_2-OMeGal as substrates are shown in Figure 3. The data are well fitted by eq (1) to give $^{16}O/^{18}O$ KIE values of 1.0188 ± 0.0006 and 1.0182 ± 0.0004 for H_2-OMeGal and D_2-OMeGal, respectively. If, as an alternative to fitting the data via eq (3), the oxygen isotope effects are calculated at each fractional conversion, the ^{18}O KIE is 1.0197 ± 0.002 for H_2-OMeGal and 1.0191 ± 0.003 for D_2-OMeGal. This approach leads to slightly larger values, with greater errors. In either case, the results show clearly that changes in oxygen bond order are occurring in the rate-determining step of $k_{cat}/K_m(O_2)$. The values for the protiated and deuterated substrates are identical within experimental error, indicating no substrate deuteration effect on the ^{18}O KIE.

4. Discussion

Demonstration of a Steady State Kinetic Ping-Pong Mechanism for Galactose Oxidase

In enzyme reactions involving multiple substrates, the kinetic mechanism can be elucidated through rate measurements in which the concentration of one substrate is varied while the alternate substrate concentrations are kept constant. This was accomplished for galactose oxidase by varying the concentration of O_2 at different fixed levels of 1-O-methyl-α-D-galactopyranoside. As illustrated in Figure 1, reciprocal plots of $k_{(app)}$ vs. $[O_2]$ at varying concentrations of H_2-OMeGal show close to parallel lines, consistent with a steady-state ping-

pong mechanism wherein the reductive and oxidative reactions half-reactions (Scheme 1) are separated by an irreversible step. A ping-pong mechanism was predicted for GAOX on the basis of stopped flow experiments,[3,4] but had not been previously shown under steady-state conditions. The values for k_{cat} and $K_m(H_2\text{-OMeGal})$, Table 1, are in agreement with literature reports of 1180 s^{-1} and 175 mM for reaction of GAOX with galactose at 20 °C and pH 7.0.[24] The value for $k_{cat}/K_m(H_2\text{-OMeGal})$ compares favorably with reported second-order rate constants in the range of 1×10^4 M^{-1}s^{-1}.[3,4] The much faster value of $k_{cat}/K_m(O_2)$, 2.6(0.3) × 10^6 m^{-1}s^{-1}, is also in the range of previously reported values for second-order rate constants of 8×10^6 M^{-1}s^{-1} at 4 °C and 1×10^7 M^{-1}s^{-1} at 25 °C.[3,4] However, prior efforts to obtain $K_m(O_2)$ for galactose oxidase were unsuccessful and it was concluded that the enzyme could not be saturated with oxygen.[24,25] In contrast to earlier steady-state work, the current experiments were conducted at 10 °C slowing the reaction sufficiently for observation of saturation kinetics with [O_2]; this results in the ability to detect the diagnostic pattern of non-intersecting lines characteristic of ping-pong kinetics, Figure 1. The experimental value for $K_m(O_2)$ reported herein is of the same order of magnitude as the concentration of dissolved oxygen in water, a not surprising result given that galactose oxidase is an extracellularly secreted enzyme.

Deuterium Kinetic Isotope Effects Indicate Retention of Substrate-Derived Deuterium in the Reduced Form of GAOX

Kinetic isotope effects were utilized to elucidate the rate-determining steps of the two half-reactions. Large deuterium isotope effects of 24 ± 1 and 32 ± 5 were observed on k_{cat} and $k_{cat}/K_m(\text{OMeGal})$ for the reductive reaction (10 °C), which can be compared to previously reported values of 21.2 and 22.5 obtained at 4 °C under conditions of low substrate concentration by stopped flow and steady-state methods, respectively. The large size of the KIE, together with the previously reported temperature dependence of this parameter, support a tunneling mechanism for H-atom abstraction from the sugar by the tyrosyl radical cofactor.[3]

Measurement of $k_{cat}/K_m(O_2)$ allows for the observation of isotope effects on the portion of a reaction that begins with the binding of oxygen through the first irreversible step of oxygen reactivity. The ability to separate the two half-reactions of GAOX, eqs. (1) and (2), would imply that deuteration of the sugar substrate will have no impact on the $k_{cat}/K_m(O_2)$ for enzyme recycling by oxygen. However, a small but real $^D(k_{cat}/K_m(O_2))$ of 1.6 to 1.9, Table 2, indicates that the deuterium abstracted from the sugar remains in the active site. The fact that the solvent isotope effect on $k_{cat}/K_m(O_2)$ is unity, together with the fact that the observed value for $^D(k_{cat}/K_m(O_2))$ is similar in H_2O and D_2O, argues that bulk solvent is not able to penetrate the active site of the reduced enzyme. The carryover of the isotope from the reductive reaction to the oxidative reaction is likely a function of the active site tryptophan (W290), which is involved in π-stacking with the Tyr-Cys cofactor.[26] Modification of this residue has been shown to dramatically slow the rate of catalysis while increasing solvent accessibility to the cofactor, as evidenced by rapid decay of the radical species.[27] It is certainly expected that solvent will be accessible to the active site during certain stages of the catalytic cycle, e.g. in the Cu(II)-TyrCys• enzyme state that forms during H_2O_2 release and substrate binding. However, the present data appear to rule out solvent access during the oxidative half reaction that involves Cu(I)-TyrCys.

By analogy to the steps proposed for the reductive half-reaction, the rate-determining step of the oxidative half-reaction is hypothesized to be an H-atom transfer from the cofactor to metal-bound superoxide. Typical KIEs for H-atom transfer reactions involving tunneling are in the range of 10-100.[28,29] One possibility for the small deuterium KIE observed herein for $k_{cat}/K_m(O_2)$ is that the hydrogen atom transfer in the oxidative half-reaction of GAOX is occurring

between two heteroatoms, O–H---O. In general, smaller primary deuterium isotope effects are anticipated for such reactions,[28] in comparison to hydrogen atom abstraction from carbon. [29] However, a value of 1.6 to 1.9 would appear outside the range anticipated for a rate-limiting O–H abstraction via tunneling, raising the possibility that the O-H bond cleavage is only partially rate-determining for the measured $k_{cat}/K_m(O_2)$.

Impact of Substrate Deuteration on Oxygen-18 Kinetic Isotope Effects Implicates a Single Rate-Limiting H-Transfer Step for Oxidation of Reduced Cofactor by O_2

The use of O-18 kinetic isotope effects to establish rate-determining steps for reactions involving O_2 has seen increasing application in the recent literature. Competitive ^{18}O kinetic isotope effects ($^{18}k_{cat}/K_m(O_2)$) were carried out for GAOX to assess the extent to which a change in oxygen bond order occurs in all reversible steps involving O_2 binding through the first irreversible step. The experimental ^{18}O KIE values for GAOX are 1.0188 ± 0.0006 and 1.0182 ± 0.0004 using H_2-OMeGal and D_2-OMeGal, respectively, Table 2. These results both identify electron transfer to O_2 as a rate-limiting step and eliminate a partially rate-determining binding of O_2 to GAOX. If the latter had been the case, the ^{18}O KIE would be predicted to increase upon substrate deuteration, as the contribution of hydrogen transfer to $k_{cat}/K_m(O_2)$ is enhanced relative to reaction with protio-substrate. The combined observations of the measured ^{18}O KIE being independent of substrate deuteration, while substrate deuteration reduces the magnitude of $k_{cat}/K_m(O_2)$, implicates a single rate-determining step for hydrogen abstraction from reduced cofactor in the oxidative half-reaction. In this manner the observed small impact of substrate deuteration on $k_{cat}/K_m(O_2)$ is concluded to be an intrinsic property of the oxidative half-reaction, in marked contrast to the enormous non-classical KIE observed for the reductive half-reaction.

One feature that will affect the size of the measured isotope effect is the reaction driving force and whether hydrogen transfer takes place from the ground state vibrational level of reactant to the ground state vibrational level of product ($0 \rightarrow 0$ transition). In the case of quite a few enzymatic reactions that catalyze hydrogen atom abstraction from carbon, the elevated size of the experimental substrate deuterium isotope effect and its weak temperature dependence can be explained via an electronically and vibronically non-adiabatic treatment in which the majority of hydrogen transfer occurs from the lowest vibrational level of the reactant. A contrasting trend has been seen in numerous hydride transfer reactions where the primary deuterium isotope effect is small and in the range of $k_H/k_D = 3$ to 4, although considerable evidence has been amassed for hydrogen tunneling in these systems as well.[30] Hammes-Schiffer and her co-workers have been able to rationalize the differences between the large isotope effects in the free radical based hydrogen atom transfers in enzymes vs. hydride transfer reactions via the use of an electronically adiabatic treatment in the latter case.[31] That is, theoretical treatment of systems in which there is substantial electronic interaction between the hydrogen donor and acceptor reproduces the small experimental isotope effects. It, thus, seems very likely that the most fundamental difference between the C-H and O-H activation steps catalyzed by GAOX lies in the degree of ground state interaction between the hydrogen donor and acceptor, with this being much greater for the half-reaction in which a hydrogen atom is removed from oxygen. The greater electronic interaction in the O-H---O transfer is also expected to decrease the heavy atom donor to heavy atom acceptor distance, which will further decrease the size of the isotope effect. Though a formal theoretical treatment of GAOX is outside the scope of this study, the present results offer the opportunity to explore how a single enzyme active site controls hydrogenic wave function overlap for an adiabatic (O-H---O) vs. non-adiabatic (C-H---O) process.

The Magnitude of the ^{18}O KIE in GAOX Provides a Frame of Reference for Oxygen Activation at a Cu^{+1} Center

A very surprising feature from this study is an O-18 kinetic isotope effect for GAOX that is remarkably close to values measured previously for DβM and PHM, Table 2, providing corroborative evidence for a reactive copper-superoxo species as the oxygenating agent in the latter enzyme systems. Inspection of $k_{cat}/K_m(O_2)$ values, under conditions where this parameter is limited by the hydrogen transfer step, indicates a ten-fold or larger rate constant for GAOX than for the copper monooxygenase family: 2.5×10^6 M^{-1}s^{-1} for GAOX vs. 0.05 to 2.6×10^5 M^{-1}s^{-1} for PHM and DβM, depending on the substrate oxidized. The faster rate for the GAOX oxidative half-reaction is in accord with model studies that have demonstrated a lower barrier for hydrogen abstraction from oxygen than carbon.[32] In addition to differences in the magnitude of $k_{cat}/K_m(O_2)$, X-ray structures for the active sites of GAOX and PHM indicate very different copper geometries, active site structures and access to bulk solvent. The fact that such different enzyme systems display almost identical values for the ^{18}O KIE establishes a value of ≥ 1.019 as a frame of reference for abstraction of a hydrogen atom at a copper superoxo- center.

As argued in previous publications, reaction of oxygen at a metal center in the absence of O-O bond cleavage may be expected to produce a kinetic isotope effect that will be fairly insensitive to the reaction coordinate frequency.[33] Under this condition, the equilibrium O-18 isotope effect can provide an estimate for the upper limit of the measured kinetic isotope effect, calculated in Table 3 for formation of Cu(II)-OOH from Cu(I) and O_2 using experimental frequencies and isotope shifts for the indicated complexes (models I and II) or DFT calculations (model III). Roth has advocated the use of DFT calculations to obtain a full-range of vibrational frequencies when estimating equilibrium O-18 isotope effects, noting that in some instances the use of the more limited experimental frequencies can lead to an over-estimate of the values for the isotope effect.[34] We consider the O-18 equilibrium isotope effects for Cu(II)(-OOH) formation within models I and II, Table 3, a reasonable starting frame of reference for the present studies, while the value for model III, Table 3, appears much too low to be relevant to the kinetic isotope effects for GAOX and PHM/DβM.

The present results are relevant to a recent study of the reaction mechanism for the oxidative half-reaction of the copper-dependent pea seedling oxidase (PSAO)[35]. The size of the ^{18}O KIE played a dominant experimental role in the conclusion of a rate-limiting outer sphere electron transfer from the reduced active site cofactor to a pre-formed Cu(II)($O_2{}^{\cdot-}$)[36]. The authors report an O-18 KIE of 1.0136, considerable smaller than the KIE data now available for GAOX and for PHM/DβM. It could be argued that the mechanism put forth for the PSAO reaction is sufficiently different from the outer sphere hydrogen atom transfer to the pre-formed Cu(II)($O_2{}^{\cdot-}$) in GAOX and PHM/ DβM, such that the O-18 may be expected to be of a different magnitude. However, as has been shown quite convincingly in previous analyses of the reductive activation of O_2, formation of a hydroperoxo anion predicts a much larger KIE than for production of hydrogen peroxide, Table 3, a result of decreased bonding to the reactive oxygen in the hydroperoxo- anion case. Thus, based on the present studies, the mechanism proposed for PSAO in ref (35) would predict an ^{18}O KIE at least as large as 1.018. It remains possible that an inner sphere oxidative half-reaction is operating in PSAO: however, the conclusion of such a mechanism based on the magnitude of the experimentally available ^{18}O KIE requires further examination.

Acknowledgment

## Abbreviations

GAOX, galactose oxidase; DβM, dopamine β-monooxygenase; PHM, peptidylglycine α-hydroxylating monooxygenase; TβM, tyramine β-monooxygenase; DFT, density functional theory; H_2-OMeGal, 1-O-methyl-β-D-galactopyranoside; D_2-OMeGal, 1-O-methyl-[6,6-$^2H_2$]-α-D-galactopyranoside; KIE, kinetic isotope effect; EIE, equilibrium isotope effect.

References

1. Rogers MS, Baron AJ, McPherson MJ, Knowles PF, Dooley DM. J. Am. Chem. Soc 2000;122:990–991.

2. Whittaker MM, Whittaker JW. J. Biol. Chem 2003;278:22090–22101. [PubMed: 12672814]

3. Whittaker MM, Ballou DP, Whittaker JW. Biochemistry 1998;37:8426–8436. [PubMed: 9622494]

4. Borman CD, Saysell CG, Sykes AG. J. Biol. Inorg. Chem 1997;2:480–487.

5. Klinman JP. Chem. Rev 1996;96:2541–2561. [PubMed: 11848836]

6. Klinman JP. J. Biol. Chem 2006;281:3013–3016. [PubMed: 16301310]

7. Chen P, Solomon EI. Proc. Natl. Acad. Sci 2004;36:13105–13110. [PubMed: 15340147]

8. Crespo A, Marti MA, Roitberg AE, Amzel LM, Estrin DA. J. Am. Chem. Soc 2006;128:12817–12828. [PubMed: 17002377]

9. Evans JP, Ahn K, Klinman JP. J. Biol. Chem 2003;50:49691–49698. [PubMed: 12966104]

10. Francisco WA, Merkler DJ, Blackburn NJ, Klinman JP. Biochemistry 1998;37:8244–8252. [PubMed: 9609721]

11. Chen P, Solomon EI. J. Am. Chem. Soc 2004;126:4991–5000. [PubMed: 15080705]

12. Prigge ST, Eipper BA, Mains RE, Amzel LM. Science 2004;304:864–867. [PubMed: 15131304]

13. Tressel P, Kosman DJ. Methods in Enzymol 1982;89:163–171. [PubMed: 6890617]

14. Amaral D, Bernstein L, Morse D, Horecker BL. J. Biol. Chem 1963;238:2281–2284. [PubMed: 14012475]

15. Hatton MWC, Regoeczi E. Methods in Enzymol 1982;89:172–176.

16. Kosman DJ, Ettinger MJ, Weinger RE, Massaro EJ. Arch. Biochem. Biophys 1974;165:456–467. [PubMed: 4441089]

17. Whittaker MM, Whittaker JW. Protein Expr. Purif 2000;20:105–111. [PubMed: 11035958]

18. Bigeleisen J, Mayer MG. J. Chem. Phys 1947;15:261–267.

19. Tian GC, Klinman JP. J. Am. Chem. Soc 1993;115:8891–8897.

20. Roth, JP.; Klinman, JP. Isotope Effects in Chemistry and Biology. Kohen, A.; Limbach, H-H., editors. Taylor and Francis Inc.; Boca Raton, FL: 2006. p. 645-669.

21. Baron AJ, Stevens C, Wilmot C, Seneviratne KD, Blakeley V, Dooley DM, Phillips SEV, Knowles PF, McPherson MJ. J. Biol. Chem 1994;269:25095–25105. [PubMed: 7929198]

22. Whittaker MM, Whittaker JW. J. Biol. Chem 1988;263:6074–6080. [PubMed: 2834363]

23. Tressel P, Kosman DJ. Anal. Biochem 1980;105:150–153. [PubMed: 7192504]

24. Kwiatkowski LD, Adelman M, Pennelly R, Kosman DJ. J. Inorg. Biochem 1981;14:209–222. [PubMed: 7196436]

25. Villafranca, JJ.; Freeman, JC.; Kotchevar, A. Bioinorganic Chemistry of Copper. Karlin, KD.; Tyeklar, Z., editors. Chapman and Hall; New York: 1993. p. 439-446.

26. Ito N, Phillips SEV, Stevens C, Ogel ZB, McPherson MJ, Keen JN, Yadav KDS, Knowles PF. Nature 1991;350:87–90. [PubMed: 2002850]

27. Rogers MS, Tyler EM, Akyumani N, Kurtis CR, Spooner RK, Deacon SE, Tamber S, Firbank SJ, Mahmoud K, Knowles PF, Phillips SEV, McPherson MJ, Dooley DM. Biochemistry 2007;46:4606–4618. [PubMed: 17385891]

28. Bell, RP. The Proton in Chemistry. Cornell University Press; New York: 1973. p. 250-296.

29. Knapp MJ, Rickert K, Klinman JP. J. Am. Chem. Soc 2002;124:3865–3874. [PubMed: 11942823]

30. Nagel ZD, Klinman JP. Chem. Rev 2006;106:3095–3118. [PubMed: 16895320]

31. Hammes-Schiffer S. Acc. Chem. Res 2006;39:93–100. [PubMed: 16489728]

32. Mayer JM. Annu. Rev. Phy. Chem 2004;55:363–390.

33. Lanci MP, Brinkley DW, Stone KL, Smirnov VV, Roth JP. Angew. Chem., Int. Ed 2005;44:7273–7276.

34. Roth JP. Curr. Opin. Chem. Biol 2007;11:142–150. [PubMed: 17307017]

35. Mukherjee A, Smirnov VV, Lanci MP, Brown DE, Shepard EM, Dooley DM, Roth JP. J. Am. Chem. Soc 2008;130:9459–9473. [PubMed: 18582059]

36. A second major argument for an inner sphere mechanism in PSAO came from a comparison of the experimental thermal activation parameters to reaction driving force using a thermodynamics cycle based on solution bond dissociation energies and pKa values. However, as the authors comment, the difference between the observed $\Delta G^{\ddagger} = 5.6 \pm 1.3$ kcal/mol and the calculated $\Delta G^{\ddagger} = 8.5$ kcal/mol for reaction of the monoanion of the reduced cofactor could be accounted for by a strategically placed counterion or protein-derived electrostatics (Ref (35)).

37. Tian GC, Berry JA, Klinman JP. Biochemistry 1994;33:226–234. [PubMed: 8286345]

38. Francisco WA, Blackburn NJ, Klinman JP. Biochemistry 2003;42:1813–1819. [PubMed: 12590568]

39. Yamaguchi S, Kumagai A, Nagatomo S, Kitagawa T, Funahashi Y, Ozawa T, Jitsukawa K, Masuda H. Bull. Chem. Soc. Jpn 2005;78:116–124.

(A)

(B)
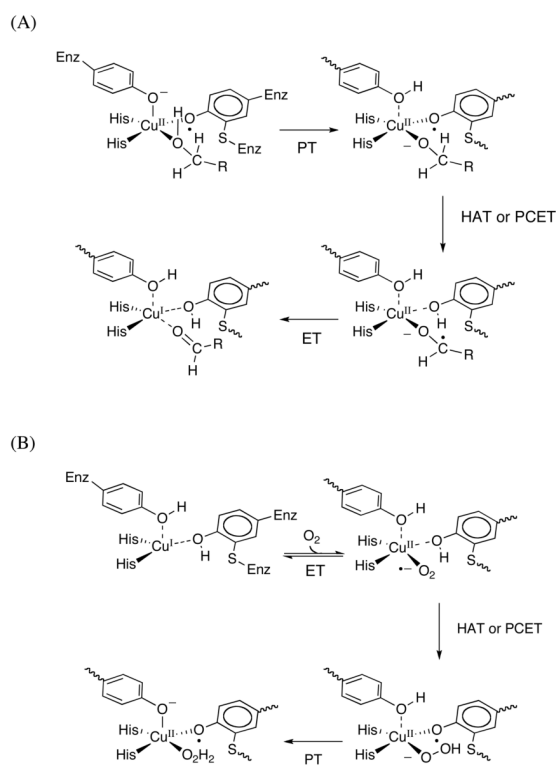
Scheme 1.
Working Chemical Mechanisms for GAOX: (**A**) Reductive Half Reaction (in which bound substrate is converted to bound product); and (**B**) Oxidative Half-Reactions of GAOX (in which free O_2 is converted to bound H_2O_2).

C-H
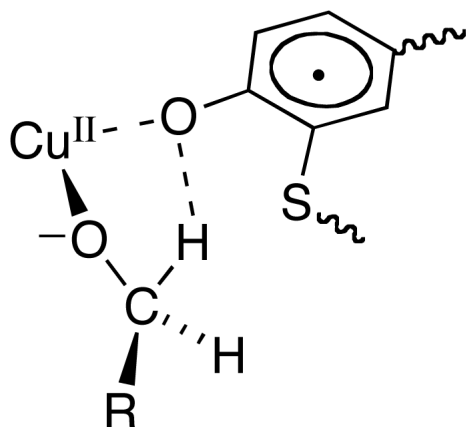
O-H
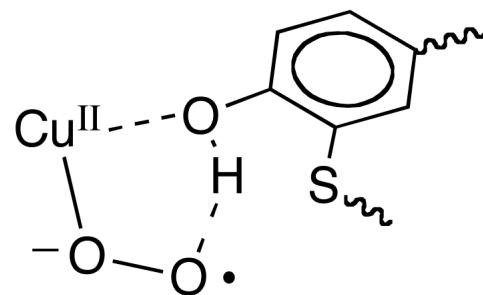
Scheme 2.
Comparison of C-H vs. O-H Activation Steps in GAOX.
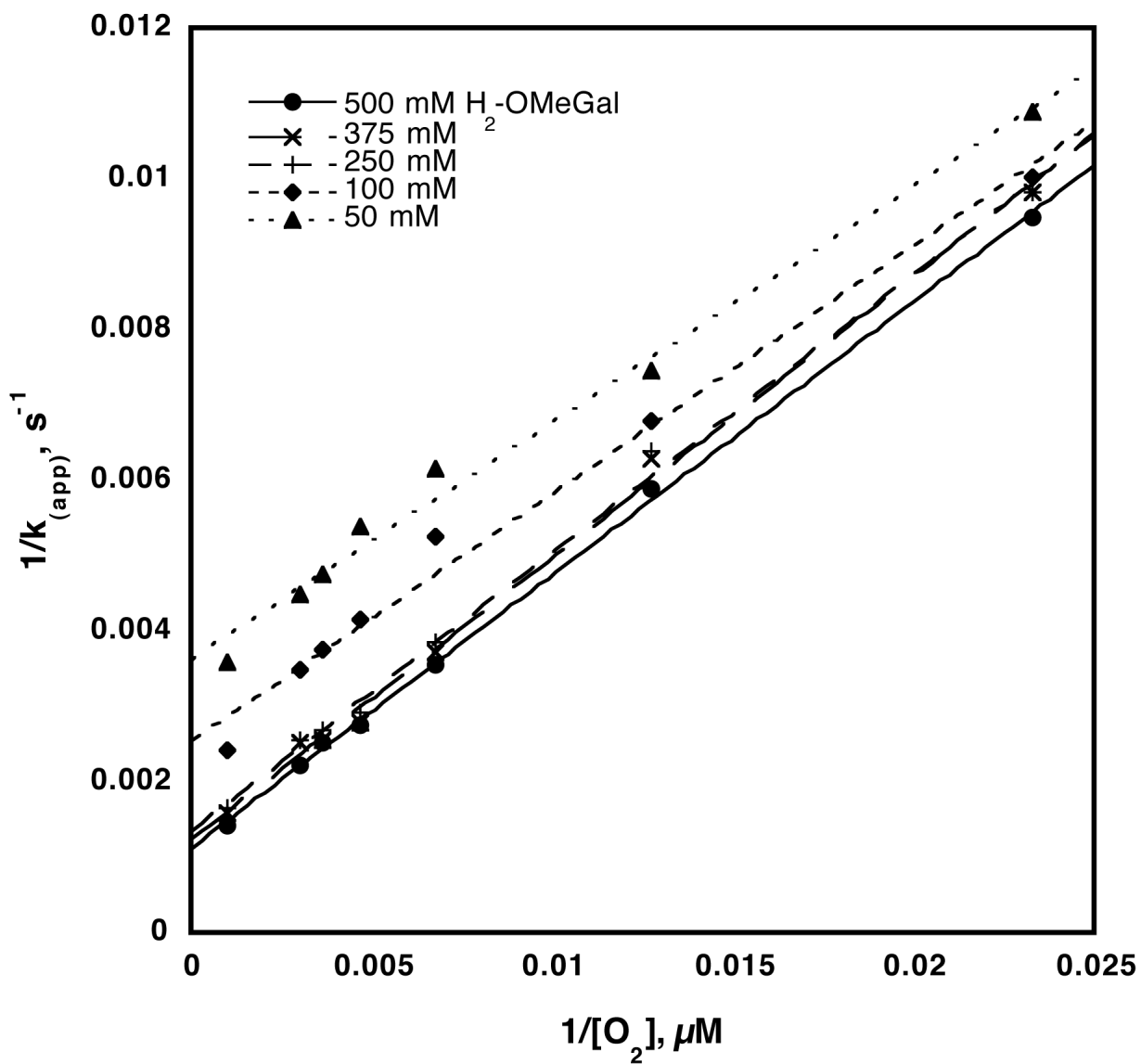
Figure 1.
Reciprocal plot of rate constants for GAOX vs. [O_2], to illustrate the ping-pong nature of the GAOX reaction. All reactions were in 50 mM sodium phosphate (pH 7.0) and 1 mM K_3Fe(CN)$_6$ at 10 °C. The average calculated value for $k_{cat}/K(O_2)$ was $2.6 \pm 0.1 \times 10^6$ $M^{-1}s^{-1}$.
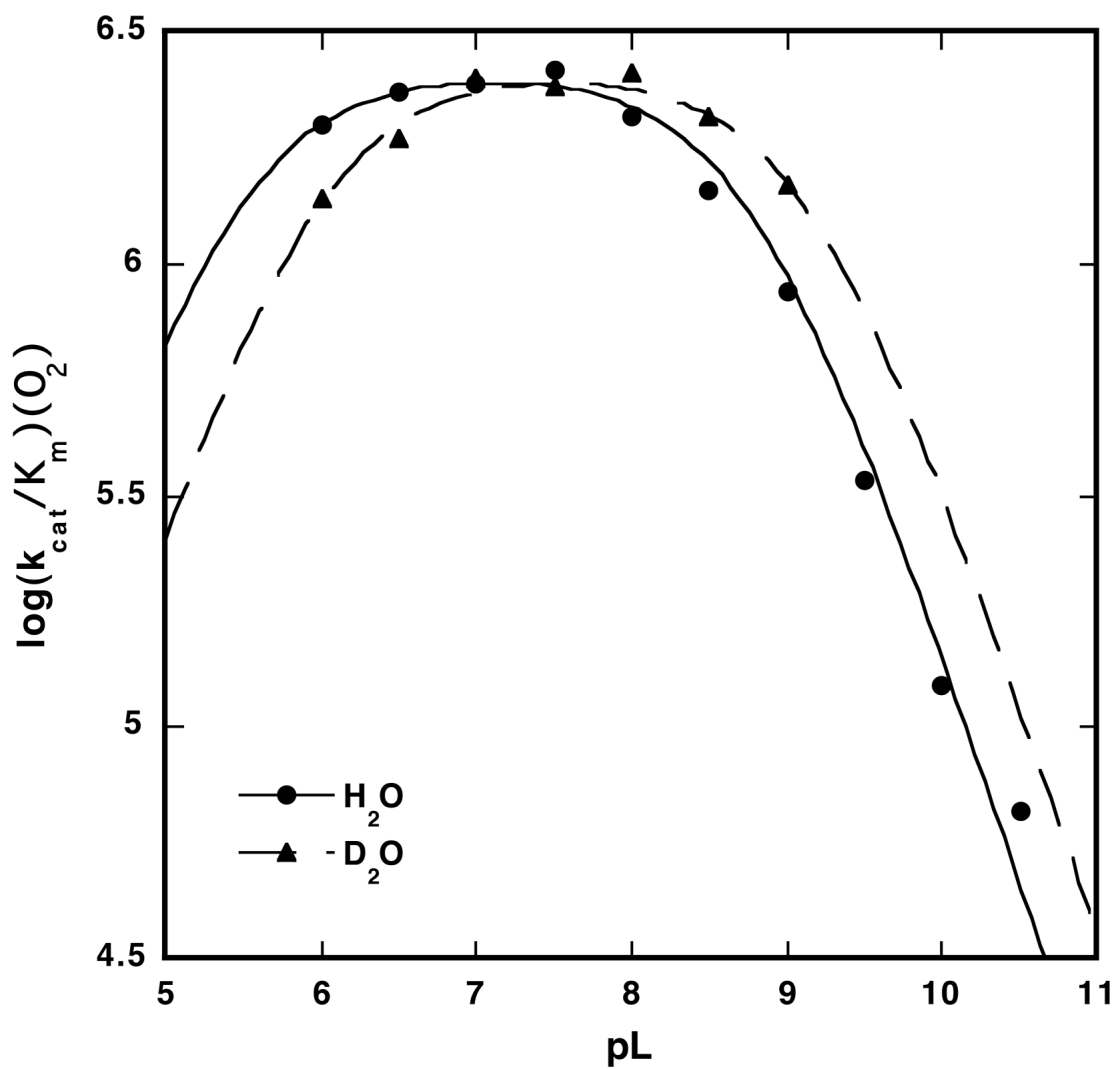
Figure 2.
Plot of $\log(k_{cat}/K_m(O_2))$ vs. pL at 10 °C. Reactions contained 200 mM H_2-OMeGal, 40-350 μM O_2, and 2 nM GAOX in a solution of 50 mM sodium phosphate and 1 mM $K_3Fe(CN)_6$.
Eq: $\log(k_{cat}/K_m) = \log(k_{cat}/K_m)_{max} - \log(1+10^{pKa_1 - pK} + 10^{pL - pKa_2})$.
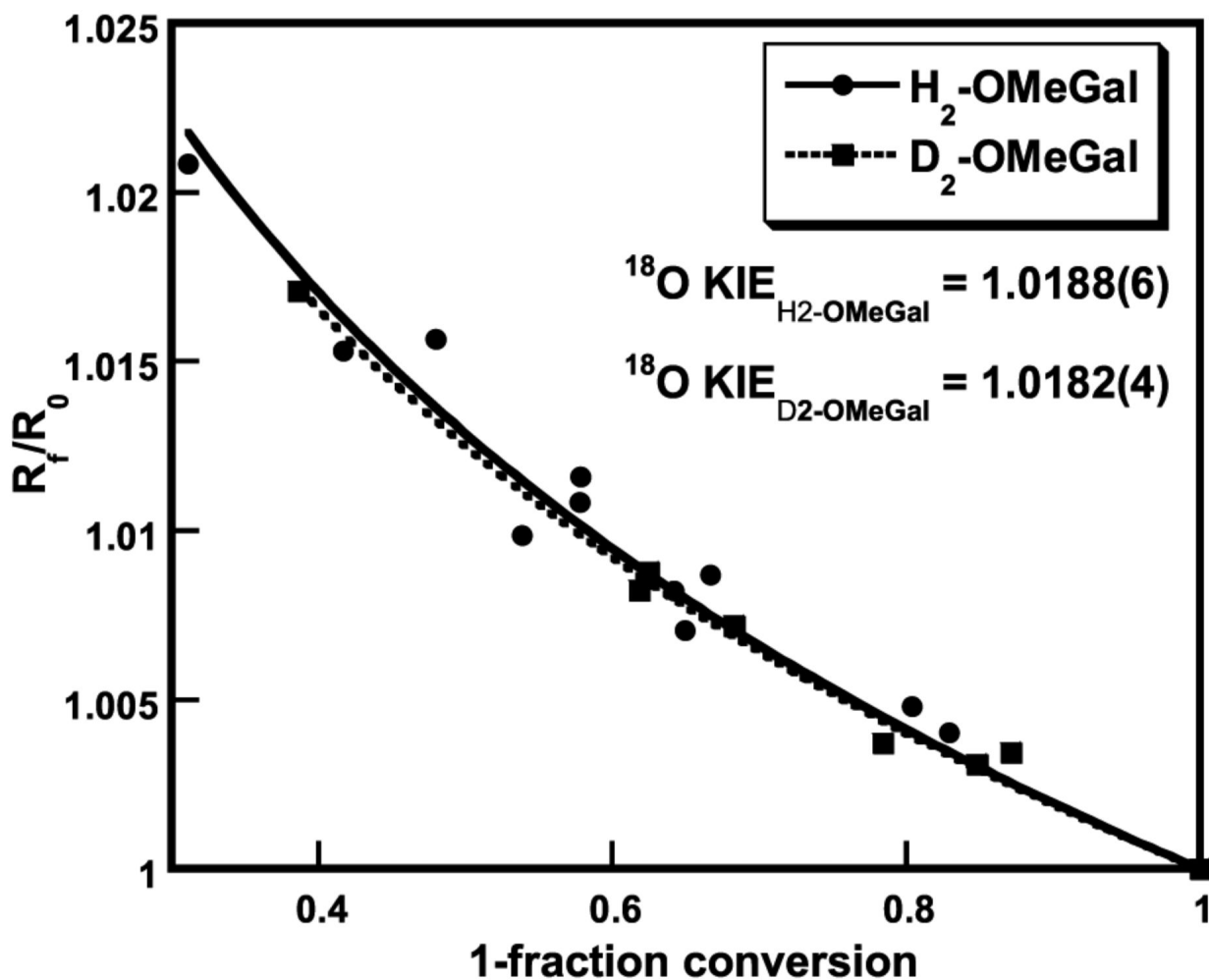
Figure 3.
Isotope fractionation plots for reaction of GAOX (10 °C, pH 7) with H_2-OMeGal (●, fit in solid line) and D_2-OMeGal (■, fit in dashed line). ^{18}O KIE values were obtained by fitting to eq. (3).

Table 1

Kinetic Parameters for GAOX at 10 °C, pH 7.0 with Protio- and Deuterio- Substrates.

Parameter	H_2-OMeGal	D_2-OMeGal
k_{cat}, s^{-1}	1165 (5)	49 (2)
k_{cat}/K_m(OMeGal), M^{-1}, s^{-1}	8.3 (0.6) $\times 10^3$	2.6 (0.4) $\times 10^2$
k_{cat}/K_m(O_2), M^{-1}, s^{-1}	2.6 (0.3) $\times 10^6$	1.5 (0.2) $\times 10^6$
K_m(OMeGal), mM	1.4 (0.1) $\times 10^2$	1.9 (0.2) $\times 10^2$
K_m(O_2), μM	4.4 (0.3) $\times 10^2$	77 (10)[a]

[a] Value was calculated from k_{cat} and k_{cat}/K_m(O_2).

Table 2

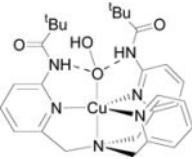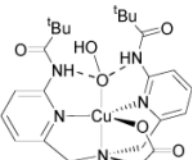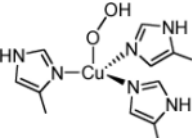Kinetic Deuterium Isotope Effects for GAOX at 10 °C, pH 7.0.

Parameter	Value
$^D k_{cat}$, s^{-1}	24 (1)
$^D(k_{cat}/K_m)$(OMeGal)	32 (5)
$^D(k_{cat}/K_m)$(O$_2$)	1.6 (0.3)
$^{D_2O}(kcat/K_m)$(O^2)[a]	1.0 (0.3)
$^{D_2O}(kcat/K_m)$(O^2)[b]	1.9 (0.7)

[a] Measured at a fixed sugar and variable O$_2$. H$_2$-OMeGal in H$_2$O vs. H$_2$-OMeGal in D$_2$O.

[b] Double isotope effect. H$_2$-OMeGal in H$_2$O vs, D$_2$-OMeGal in D$_2$O.

Table 3

Comparison of Measured and Calculated Kinetic and Equilibrium O-18 Isotope Effects

System	^{18}O KIE (Exptl)	^{18}O EIE (Calculated)
Enzymes:		
DβM	1.0214 to 1.0256[a]	---
PHM	1.0212[b]	---
GAOX	1.0188 (0.0006)[c]	---
Model systems:		

$$Cu^{I} + O_2 \underset{}{\overset{e^-,\, H^+}{\rightleftharpoons}} Cu^{II}\text{-OOH}$$

System	^{18}O KIE (Exptl)	^{18}O EIE (Calculated)
I (bppa)Cu^{II}-OOH	---	1.0253[d]
II (bpga)Cu^{II}-OOH	---	1.0258[d]
III (MeIm)$_2$(δ-MeIm)Cu^{II}-OOH	---	1.0125[e]
$O_2 \underset{}{\overset{2e^-,\, H^+}{\rightleftharpoons}} \text{H-O-O}^-$	---	1.034[f]
$O_2 \underset{}{\overset{2e^-,\, 2H^+}{\rightleftharpoons}} H_2O_2$	---	1.011[f]

[a] Ref (37).

[b] Ref (38).

[c]This work.

[d]18O EIEs calculated using O-O and Cu-O frequencies and isotope shifts from Ref 39; these 18O EIEs values may be overestimated by using only a few isotopic frequencies.

[e]Ref (35).

[f]Ref (19).